Supporting information for:

Polyamidoxime grafting ultrahigh-strength cellulose-based jute fabric for highly effectively extracting uranium from seawater

Zhiming Mi [a], Dexing Zhang [a], Junman Wang [a], Shiman Bi [a], Jing Liu [a], Xiyu Gao [a], Dawei Zhang [b], Yuanping Jiang [a], Zuojia Li [a], Yean Zhu [c], Zhixiao Liu [a,*]

[a] *Jiangxi Province Key Laboratory of Polymer Micro/Nano Manufacturing and Devices, East China University of Technology, Nanchang, 330013, PR China.*

[b] *College of Chemistry and Pharmaceutical Engineering, Jilin Institute Chemical Technology, Jilin City 132022, China.*

[c] *Jiangxi Province Key Laboratory of Synthetic Chemistry, East China University of Technology, Nanchang, Jiangxi 330013, China.*

Correspondence to: Zhixiao Liu (E-mail: lzx@ecut.edu.cn).

Content

1. Materials

Jute fabric (80#) was provided by Jinhua Science and Technology Co., Ltd. (Zhejiang, China). Polyacrylonitrile (PAN, 99%, Mw=150,000) was purchased from BASF Co. (Germany) and dried at 150 °C for 24 h prior to use. *N, N*-Dimethylformamide (DMF, 99.8%), hydroxylamine hydrochloride (NH_2OH HCl, 98.5%), sodium hydroxide (NaOH, 96%), 1,3,5-benzenetricarbonyl trichloride (TMC, 98 wt%) and arsenazo III ($C_{22}H_{18}As_2N_4O_{14}S_2$, 98%) were supplied by Sinopharm Chemical Reagent Beijing Co. Ltd. $Ni(NO_3)_2$ $6H_2O$ (99%), $Pb(NO_3)_2$ $6H_2O$ (99%), $Zn(NO_3)_2$ $6H_2O$ (99%), $Co(NO_3)_2$ $6H_2O$ (99%), $Fe(NO_3)_2$ $6H_2O$ (99%), $Cu(NO_3)_2$ $6H_2O$ (99%), $NaVO_3$ (99%), and $UO_2(NO_3)_2$ $6H_2O$ were all bought from Macklin Biochemical Co., Ltd. (Shanghai, China) and used directly. Ethanol (C_2H_5OH, 95%), hydrochloric acid (HCl, 12 mol/L), hydrogen peroxide (H_2O_2, 30 wt%), nitric acid (HNO_3, 98%) and dichloromethane (DCM) were supplied by Aldrich Chemical Co. (Shanghai, China) and used as received. Deionized water was obtained from the hollow fiber reverse osmosis device and used throughout the experiments. The other commercially available solvents and reagents were obtained from Xilong Chemical Reagent Guangdong Co. Ltd. and used without further purification.

2. Characterization

FTIR spectra were performed on a Thermal Scientific Nicolet 380 spectrometer at a resolution of 4 cm^{-1} in the range of 500–4000 cm^{-1}. The ^1H NMR spectra were conducted on a BRUKER-300 spectrometer (300 MHz) using tetramethylsilane (TMS) as the internal standard and deuterated dimethylsulfoxide (DMSO-d_6) as the solvent. X-ray photoelectron spectra (XPS) were recorded on a ESCALAB 250 (Thermo Fisher Scientific). The morphologies of jute were investigated with field emission electron microscope (FESEM, NOVA NANOSEM 450). The element distribution of the fiber surface was assessed by energy-dispersive spectrometer (EDS) equipped on the aforementioned FESEM. Differential scanning calorimetric (DSC) analysis was recorded on a TA instrument DSC Q2000 at a scanning rate of 10 °C/min from 50 °C

to 350 °C under nitrogen. Thermo gravimetric analysis (TGA) was carried out on a Netzsch STA2500 under nitrogen atmosphere at a heating rate of 10 °C min^{-1} from 100 °C to 820 °C. UV-Vis absorption tests were conducted on a spectrophotometer (UV1800PC, Shanghai, China). The surface charge of Jute-TMC-PAO was obtained by measuring the streaming potential with a SurPASS electrokinetic analyzer (Anton Paar GmbH, Austria). The pH values were recorded by a pH meter (PHSJ-3F, Shandong, China). For adsorption selectivity of Jute-TMC-PAO, the inductively coupled plasma mass spectrometry (ICP-Mass, Element 2, Thermo Fisher Scientific) was employed to assess the adsorption amounts of uranium and other competing ions after microwave digestion of the fabric.

3. Mechanical test of Jute-TMC-PAO

Mechanical properties were measured via a CNT8102 universal testing apparatus (MTS systems China Co. Ltd.). According to ASTM D3882 standard, for tensile test of Jute-TMC-PAO fiber, each fiber having 100 mm (4.0 in.) length was cut and was selected for this test. As depicted in Figure S4, jute was glued to the paper window with the help of scotch tape (Figure S4A). After curing, the sample was carefully clamped between two jaws. Before the test started, the lateral part of the paper was cut off (Figure S4B). The experiment was carried out using 25 fibers and tensile strength (T_S) was calculated by the average of five clusters. The gauge length, crosshead speed, and prestress were kept constant as 25 mm (1.0 in.), 10 mm/min, and 10 N, respectively.

4. Adsorption procedure

In this study, the adsorption experiments of Jute-TMC-PAO were mainly carried out in three situations, namely, adsorption performance in uranium aqueous solution, adsorption performance in uranium-spiked simulated seawater and adsorption performance in simulated natural seawater. Taking the adsorption performance in uranium aqueous solution as an example. As shown in Figure S5, a piece of Jute-TMC-PAO fabric with an average size of 10×10×4 mm^3 (10 mg) was packed between the diaphragms, and an aqueous uranium solution with an initial concentration of 8 ppm

cyclically flowed through the fabric (15 L/h). When the adsorption was complete, the adsorbed uranium amount was determined by UV-Vis spectrophotometer. For detailed steps, see Section VI of the Supporting Information: *Determination of uranium concentration in uranium-spiked pure water or uranium-spiked simulated seawater*. Note: all the experiments were repeated for three times, and the average adsorption data was adopted as the final reliable results.

5. Equations

Equation S1:

$$\frac{t}{q_t} = \frac{1}{k_2 q_e^{\,2}} + \frac{t}{q_e} \qquad (1)$$

Where q_t (mg/g) and q_e (mg/g) are the uranium-adsorbed amounts of Jute-TMC-PAO at the contact time and adsorption equilibrium time, respectively. t (min) is the contact time and k_2 (g/(mg min)) is the rate constant.

Equation S2:

$$\ln(q_e - q_t) = \ln q_e - k_1 t \qquad (2)$$

Where q_t (mg/g) and q_e (mg/g) are the uranium-adsorbed amounts at the contact time and adsorption equilibrium time, respectively. t (min) is the contact time and k_1 (min^{-1}) is the rate constant.

Equation S3:

$$K_d = \frac{(C_0 - C_e)}{C_e} \times \frac{V}{m} \qquad (3)$$

Where C_0 (mg L^{-1}) is the initial concentration of uranium, C_e (mg L^{-1}) is the concentration at equilibrium, V is the volume of simulated seawater (mL), and m is the mass of the Jute-TMC-PAO (g).

Equation S4 and Equation S5

$$\frac{C_e}{q_e} = \frac{C_e}{q_m} + \frac{1}{k_L q_m} \qquad (4)$$

$$q_e = k_F C_e^{\frac{1}{n}} \qquad (5)$$

Where C_e (mg/L) and q_e (mg/g) are separately the uranium concentrations in the simulated seawater and the uranium adsorption amounts of the adsorbent at equilibrium; q_m (mg/g) is the adsorption capacity; k_L (L/mg) is the Langmuir adsorption constants; k_F and n are the Freundlich adsorption constants.

6. Determination of uranium concentration in uranium-spiked pure water or uranium-spiked simulated seawater

Arsenazo (III) is a common agent for detecting uranium, and it can form a stable complex with uranyl and the complex have a specific absorption peak at the wavelength of 652 nm in UV-Vis, and the absorbance has a linear relationship with the concentration of uranyl ions within a certain range. For the standard curve of uranium-spiked pure water, we configured the uranium concentration to be 0, 5 ppm, 10 ppm, 15 ppm, 20 ppm, 25 ppm, 30 ppm, 35 ppm, 40 ppm, 45 ppm, 50 ppm, respectively. For the standard curve of uranium-spiked simulated seawater, we configured the uranium concentration to be 0, 5 ppm, 10 ppm, 15 ppm, 20 ppm, 25 ppm, 30 ppm, 35 ppm, 40 ppm, 45 ppm, 50 ppm, respectively. Afterwards, 0.5 mL HCl, (0.1 mol/L), 1 mL arsenazo (III) (0.5 g/L), and 0.5 mL uranium spiked pure water (simulated sea water) was transferred into a quartz cuvette, and then the absorbance of each standard uranium solution was measured at the fixed wavelength of 652 nm. The absorbance-concentration linear regression equation can be obtained through linear fitting. By measuring the absorbance of the test solution, the uranium concentration can be calculated by the above linear equation.

7. Figures

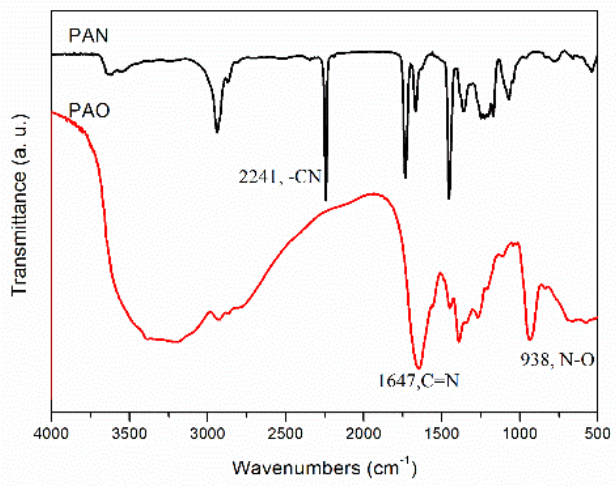

Figure S1 FTIR spectra of PAN and PAO.

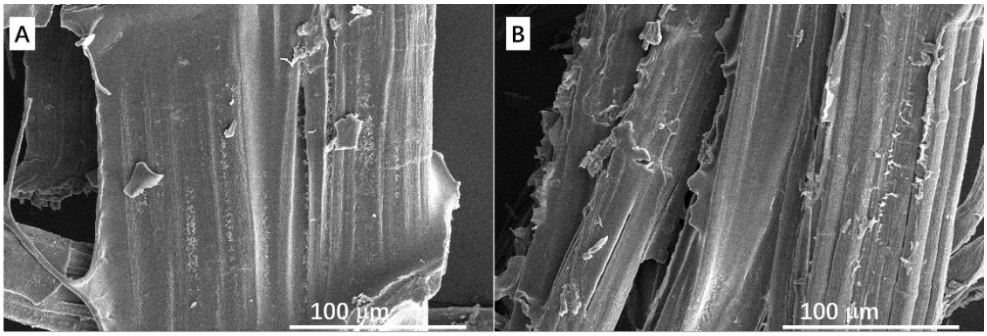

Figure S2 SEM imagines of Jute-TMC-PAO with the PAO concentrations at 5 wt% (A), 7 wt% (B), respectively.

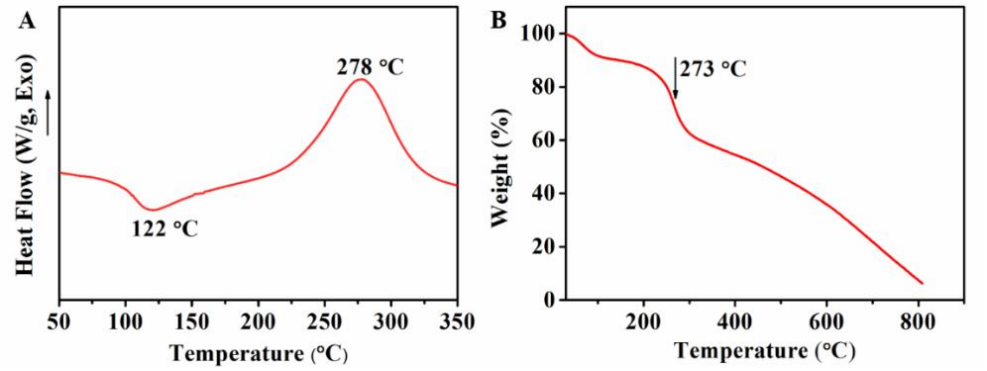

Figure S3 DSC (A) and TGA (B) curves of PAO.

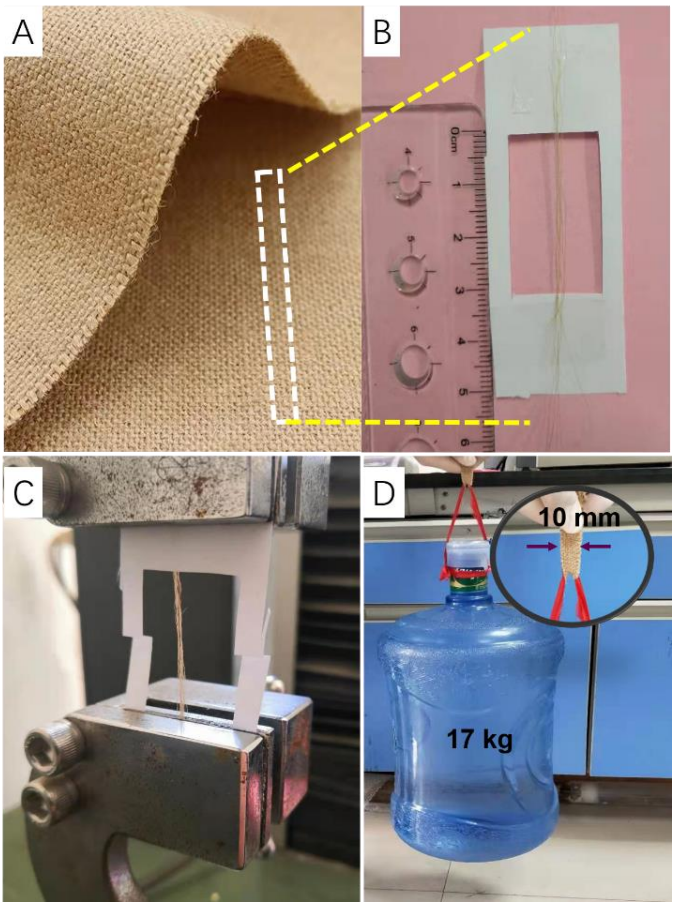

Figure S4 Picture of Jute-TMC-PAO (A). Schematic representation of the paper frame (B). Imagine of mechanical measurement apparatus based on ASTM D3882 standard (C). Schematic diagram of Jute-TMC-PAO fabric that can withstand a 17 kg barrel of drinking water (D), insert: indication of the fabric with the width at 10 mm.

① Storage tank; ② Pump; ③ Pressure indicator; ④ Jute-TMC-PAO carpet; ⑤ Diaphragm clamping.

Figure S5 Apparatus for uranium adsorption in uranium spiked water/seawater.

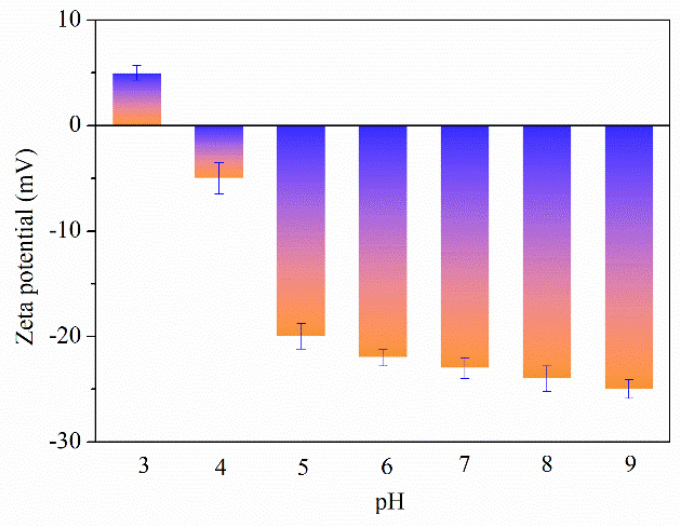

Figure S6 Zeta potential of Jute-TMC-PAO.

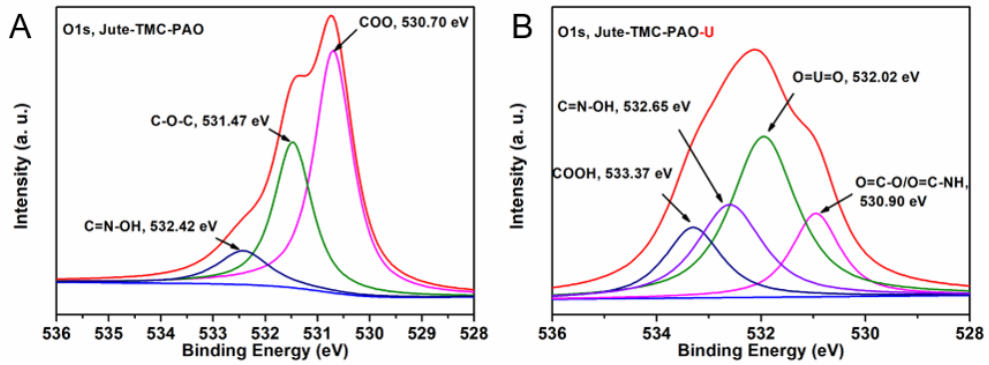

Figure S7 High resolution XPS spectra of O1s of Jute-TMC-PAO before (A) and after uranium adsorption (B).

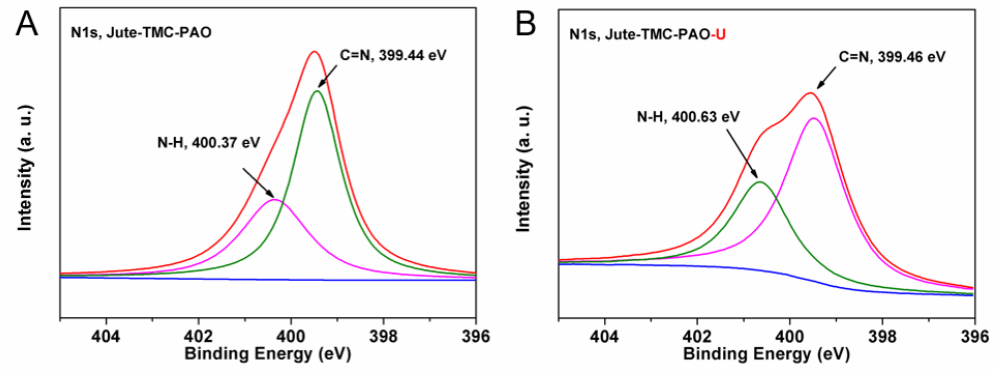

Figure S8 High resolution XPS spectra of N1s of Jute-TMC-PAO before (A) and after uranium adsorption (B).

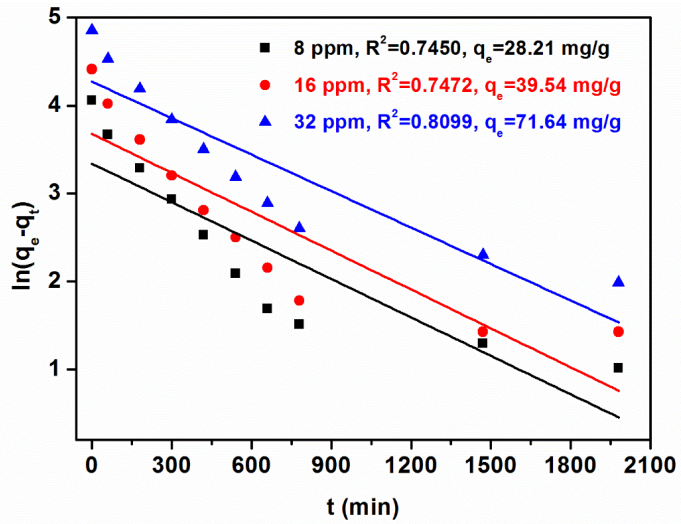

Figure S9 The fitting curves of $\ln(q_e-q_t)$ to the contact time.

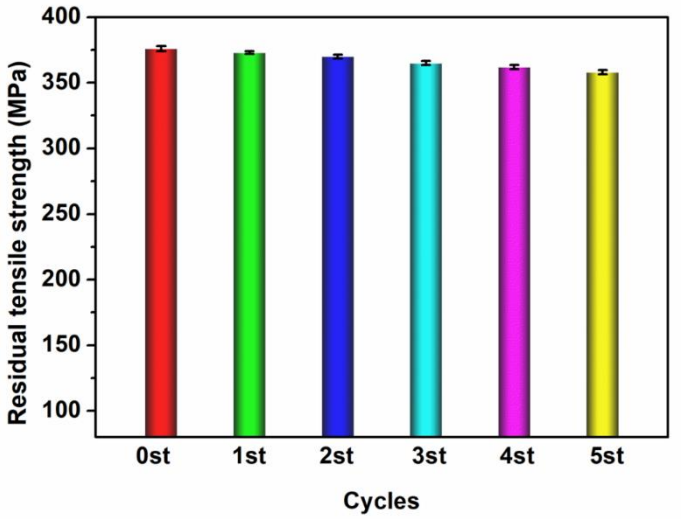

Figure S10 Residual tensile strength of Jute-TMC-PAO in five adsorption-desorption cycles.

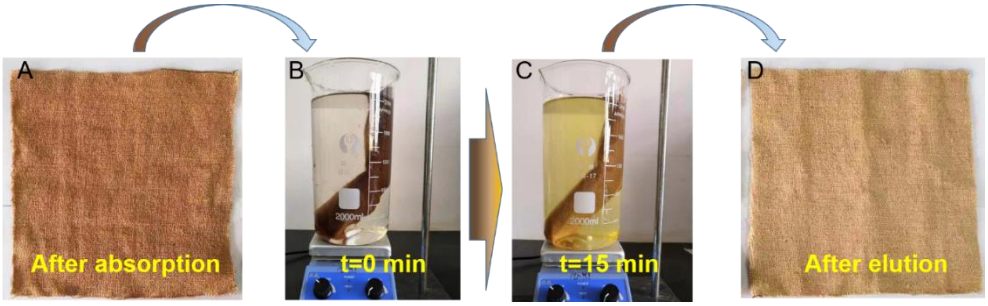

Figure S11 Color variations of Jute-TMC-PAO fabrics after uranium adsorption (A) and after desorption (D); Images of Jute-TMC-PAO fabric before (B) and after (C) uranium desorption within 15 min in 2 L of Na_2CO_3+H_2O_2 solution; Note: the square fabric (250×250×4 mm^3) was rolled up to facilitate large-scale adsorption-desorption test.

① Storage tank full of simulated natural seawater; ② Pump; ③ Pressure indicator; ④ Jute-TMC-PAO fabric; ⑤ Diaphragm clamping; ⑥ Recovery tank

Figure S12 Apparatus for uranium adsorption in simulated natural seawater. Photographs of test device (A), model diagram (B)

8. Tables

Table S1 Tensile performance of virgin jute, alkali-treated jute, and Jute-TMC-PAO.

Sample	Tensile results		
	T_S (MPa)	T_M (GPa)	E_B (%)
Virgin jute	672	4.21	11.29
Alkali-treated jute	258	1.28	13.24
Jute-TMC-PAO	376	2.76	12.80

Table S2 Ion concentration distributions in simulated seawater [a] and 100× simulated seawater.

Ions	Concentration in simulated natural seawater (ppb)	Concentration in 100× simulated seawater (ppb)
Ni	1.0	100
Pb	0.03	3
Zn	4.0	400
Co	0.1	10
Fe	1.0-2.0	150
Cu	1.3	130
V	1.5~2.4	200
U	3.3	330
Mg	1.2	120
Ca	0.35×10^6	0.35×10^6
K	0.6×10^6	0.6×10^6
Na	9.0×10^6	9.0×10^6

[a]: The simulated seawater was obtained by dissolving 0.3627 g of sea salt in 10 L of deionized water, and followed by being filtered with a 0.22 μm Teflon® membrane to obtain simulated sea water.

Table S3 Distribution coefficient and adsorption kinetic parameters.

C_0 (ppm)	K_d (mL/g)	Pseudo second order			Pseudo first order		
		R^2	q_e (mg/g)	k_2 (g/(mg min))	R^2	q_e (mg/g)	k_1 (/min)
8	1.0×10^4	0.9976	58.03	1.79×10^{-4}	0.7450	28.21	1.46×10^{-2}
16	0.6×10^4	0.9979	82.51	1.32×10^{-4}	0.7472	39.54	1.47×10^{-2}
32	0.5×10^4	0.9966	128.37	6.31×10^{-5}	0.8099	71.64	1.38×10^{-2}

Table S4 Langmuir and Freundlich models parameters.

Langmuir model			Freundlich model		
R^2	q_m (mg/g)	k_L (L/mg)	R^2	k_F	n
0.9760	171.26	0.05827	0.8784	31.8702	2.7012

Table S5 Performance of representative biobased adsorbents

Samples	Experimental conditions	Absorption capacity	References
ATMP-Sisal-150	10 ppm, uranium spiked seawater (pH=8)	16	Tellería et al., 2020
PAO-CFs membrane	2-20 ppm, deionized water (pH=5)	52.88	Wang, Zhang et al., 2020
Grafted Cellulose (SGC).	100 ppm, deionized water (pH=6)	105	Kouraim et al., 2020
Cellulose acetate adsorbent	100-700 ppm, deionized water (pH=2)	125	Hassanin et al., 2021
Urea onto cellulose (UIC)	25-300 ppm, acid solution (pH=0.1~3)	82	Ahmed et al., 2019
Carboxymethyl cellulose microsphere	25 ppm, deionized water (pH=5)	12.08	Wu et al., 2016
Amine Functionalized cellulose	150 ppm, deionized water (pH=5)	150	Yousif et al., 2015
HF-PEI-GDAC	0-400 ppm, deionized water (pH=7)	158.22	Bai et al., 2020
Fe_2O_3 impregnated cellulose beads	5-45 ppm, deionized water (pH=7)	7.6	Rule et al., 2014
Amine-impregnated cellulose	25-350 ppm, deionized water (pH=7)	56.5	Orabi et al., 2016)
Cellulose/ p-toluidine	10-110 ppm, deionized water (pH=10.5)	80	Dacrory et al., 2020
Jute-TMC-PAO	4-80 ppm, 250 mL, pH=8, seawater	171.26	**This work**

9 References

Bai, Z.H., Liu, Q., Zhang, H.S., Liu, J.Y., Yu, J., Wang, J. (2020). A novel 3D reticular anti-fouling bio-adsorbent for uranium extraction from seawater: Polyethylenimine and guanidyl functionalized hemp fibers. Chem. Eng. J. 382, 122555. https://doi.org/10.1016/j.cej.2019.122555.

Dacrory, S., Haggag, E.S.A., Masoud, A.M., Abdo, S.M., Eliwa, A.A., Kamel, S. (2020). Innovative synthesis of modified cellulose derivative as a uranium adsorbent from carbonate solutions of radioactive deposits. Cellulose, 27, 7093-7108. https://doi.org/10.1007/s10570-020-03272-w.

Hassanin, M.A., El-Gendy, H.S., Cheira, M.F., Atia, B.M. (2021). Uranium ions extraction from the waste solution by thiosemicarbazide anchored cellulose acetate. Int. J. Environ. An. 101, 351-369. https://doi.org/10.1080/03067319.2019.1667984.

Kouraim, M.N., Hagag, M.S., Ali, A.H. (2020). Adsorption of uranium from its aqueous solutions using activated cellulose and silica grafted cellulose. Radiochim. Acta. 108, 261-271. https://doi.org/doi:10.1515/ract-2019-3149.

Orabi, A.H. (2019). Synthesis of a cellulose derivative for enhanced sorption and selectivity of uranium from phosphate rocks prior to its fluorometric determination. Int. J. Environ. An. Ch. 99, 741-766. https://doi.org/10.1080/03067319.2019.1609462.

Orabi, A.H., El-Sheikh, E.M., Saleh, W.H., Youssef, A. O., El-Kady, M. Y., Shalaby, Z.M. (2016). Potentiality of uranium adsorption from wet phosphoric acid using amine-impregnated cellulose. J. Radiat. Res. Appl. Sc. 9, 193-206. https://doi.org/10.1016/j.jrras.2015.12.003.

Rule, P., Balasubramanian, K., Gonte, R.R. (2014). Uranium(VI) remediation from aqueous environment using impregnated cellulose beads. J. Environ. Radioactiv. 136, 22-29. https://doi.org/10.1016/j.jenvrad.2014.05.004.

Tellería N.A., Talavera-Ramos, W., Santos, L.D., Arias, J., Kinbaum, A., Luca, V. (2020). Functionalized natural cellulose fibres for the recovery of uranium from seawater. RSC Adv. 10, 6654-6657. https://doi.org/10.1039/D0RA00601G.

Wang, Y., Zhang, Y., Li, Q., Li, Y., Cao, L., Li, W. (2020). Amidoximated cellulose fiber membrane for uranium extraction from simulated seawater. Carbohydrate Polymers, 245, 116627. https://doi.org/https://doi.org/10.1016/j.carbpol.2020.116627.

Wu, L.P., Lin, X.Y., Du, X. C., Luo, X.G. (2016). Biosorption of uranium(VI) from aqueous solution using microsphere adsorbents of carboxymethyl cellulose loaded with aluminum(III). J. Radioanal. Nucl. Ch. 310, 611-622. https://doi.org/10.1007/s10967-016-4859-5.

Yousif, A.M., El-Afandy, A.H., Wahab, G.M.A., Mubark, A. E., Ibrahim, I.A. (2015). Selective separation of uranium(VI) from aqueous solutions using amine functionalized cellulose. J. Radioanal. Nucl. Ch. 303, 1821-1833. https://doi.org/10.1007/s10967-014-3688-7.